

# A Multiferroic Molecular Magnetic Qubit

Alexander I. Johnson,<sup>a</sup> Fhokrul Islam,<sup>b</sup> Carlo M. Canali<sup>b</sup> and Mark R. Pederson<sup>c</sup>

<sup>a</sup> Department of Physics, Central Michigan University, Mt. Pleasant, MI 48859

<sup>b</sup> Department of Physics and Electrical Engineering, Linneaus University, Kalmar, Sweden and

<sup>c</sup> Department of Physics, University of Texas El Paso, El Paso, TX 79968

(Dated: May 24, 2022)

The chiral  $Fe_3O(NC_5H_5)_3(O_2CC_6H_5)_6$  molecular cation, with  $C_3$  symmetry, is composed of three six-fold coordinated spin-carrying  $Fe^{3+}$  cations that form a perfect equilateral triangle. Experimental reports demonstrating the spin-electric effect in this system also identify the presence of a magnetic uni-axis and suggest that this molecule may be a good candidate for an externally controllable molecular qubit. Here we demonstrate, using standard density-functional methods, that the spin-electric behavior of this molecule could be even more interesting as there are energetically competitive reference states associated with both high and low local spins ( $S=5/2$  vs.  $S=1/2$ ) on the  $Fe^{3+}$  ions. Each of these structures allow for spin-electric ground states. We find that qualitative differences in the broadening of the  $Fe(2s)$  and  $O(1s)$  core levels, shifts in the core-level energies, and the magnetic signatures of the single-spin anisotropy Hamiltonian may be used to confirm whether a transition between a high-spin manifold and a low spin manifold occurs.

PACS numbers: 31.15.Ar, 31.70.Hq, 34.70.+e, 84.60.Jt, 87.15.Mi

Keywords: Molecular Magnets, Density-Functional Methods

## I. INTRODUCTION AND MOTIVATION

Molecules composed of spin carrying metal centers are ubiquitous in nature and play important roles in inorganic chemistry and biophysics. Such systems are used to transport oxygen, convert water into oxygen and hydrogen [1–4], and convert nitrogen to ammonia. The spin-spin and spin-orbit interactions associated with the heavier transition metal ions can provide non-destructive spectroscopic probes for understanding such chemical rearrangements [5]. Further, the magnetic and spin-electric behaviors of these molecules suggest they are interesting candidates from the standpoint of quantum sensing, development of classical information storage systems, and also as possible qubits for quantum information applications [6–9]. While either integer or half-integer systems could be relevant to classical information storage systems, an analysis based upon a single-J Heisenberg Hamiltonian identifies triangular transition-metal complexes

Two primary types of collective behaviors present themselves in molecules when inversion symmetry is absent. For molecules that contain metal ions with large moments (more than two unpaired electrons per site) and relatively strong exchange-coupling, the entire molecule behaves as a single spin at temperatures that are small compared to inter-ionic exchange coupling. If such molecules have uniaxial symmetries, spin-orbit coupling determines the magnitude and sign of  $D$  in the single-spin Hamiltonian ( $H_A = DS_z^2$ ). [10–17] If  $D$  is negative, the system exhibits easy axis, e.g. quasiclassical, magnetic behavior. If  $D$  is positive, the system exhibits easy-plane magnetic behavior. If easy-axis magnetic behavior is observed in these systems, the molecule is often referred to as a Type-1 molecular magnet or as an anisotropic molecular magnet. The quantum states of such molecules can

be switched through the application of magnetic fields that are integer multiples of the anisotropy parameter ( $D$ ). [12, 13]

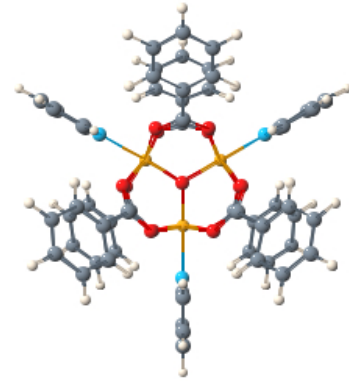


FIG. 1: The  $(Fe^{+3})_3O^{-2}(NC_5H_5)_3(O_2CC_6H_5^{-1})_6$  molecular cation is shown above. Three Fe ions form a perfect equilateral triangle with an oxygen anion in the center of the molecule. Each of three equivalent Fe ions is coordinated by the central oxygen anion, four oxygen anions associated with two four different but symmetrically equivalent carboxylate groups ( $OOC-C_6H_5$ ) and one  $NC_5H_5$  ligand.

Until recently, and in contrast to Type-1 molecular magnets, Type-2 molecular magnets or spin systems have been primarily found in complexes containing an odd number of metal ions that have small moments (one unpaired electron per site) [18–25]. For this case, higher-energy charge-transfer states between pairs of metal centers, otherwise known as the upper Hubbard band, are also coupled to the ground state by the spin-orbit interaction. This type of spin-orbit effect is generally referred

to as the Dzyalinskii-Moriya (DM) interaction [26, 27] or antisymmetric exchange interaction. The occurrence of a lack of inversion symmetry, and frustrated spin ordering provides a very different type of emergent behavior than what is observed in Type-1 molecular magnets. Moreover, because there are multiple low-energy degenerate spin-ordered configurations, each of which lead to a net dipole moment, these systems exhibit the spin-electric effect. The spin-electric effect, introduced in Refs. [6, 20] arises when the spin-ordering in an equilateral triangle changes from having three ferromagnetically ordered spins to one of the frustrated configurations with two parallel and one anti-parallel spin on their respective ions. For the remainder of this paper we refer to the non-ferromagnetically ordered configurations as either antiferromagnetic (AF) or frustrated. Shortly after the paper by Triff *et al* [20], Islam *et al* quantified the behavior of these systems using the NRLMOL suite of codes and calculated the DM interaction using density-functional theory. [21, 22] This interaction is eventually reduced to  $H_{DM} = \Delta_{Spin-Orbit} C_z S_z$  where  $C_z$  is the chirality operator and  $\Delta_{Spin-Orbit}$  is a constant that depends on the spin-orbit interaction between the upper and lower Hubbard bands in the half-filled three-site  $C_3$  system. The result is that the chiral and antichiral states with the same  $M_s$  are split by  $2\Delta_{Spin-Orbit}$ . For a sufficiently large spin-orbit interaction this leads to a ground-state doublet composed of a chiral  $M_s = \frac{1}{2}$  and anti-chiral  $M_s = -\frac{1}{2}$  that can behave as a qubit.

The experimental demonstration of the spin-electric effect has occurred only recently. For example, Plass *et al* [9] and Boudalis *et al* [23] have experimentally identified Cu-based and Fe-based molecular spin qubits in which the transition metal ions are found on a triangular lattice in molecules with perfect  $C_3$  symmetry. These papers reiterate the need to construct such a qubit from metal ions that contain half-integer electron spin ( $S_{loc} = \frac{2K+1}{2}$ ) since, as also outlined below, such systems lead to a ground state with a total spin of  $S_{tot} = \frac{1}{2}$ .

To date, most Type-2 molecular magnets, such as the one recently identified by Plass *et al* [9], have been composed of metal ions that tend to carry small moments (e.g. Cu and V). However, the Fe-based system [23], introduced by Boudalis *et al*, is interesting due to the observations of the magneto-electric coupling in a qubit composed of high-spin ( $S_{loc} = \frac{5}{2}$ ) metal centers. By subjecting the molecule to an electric field that is parallel to the plane of the three iron atoms, they have demonstrated that the ground state couples to the externally applied electric field and comment that their work is the first experimental confirmation of the spin-electric effect. Boudalis *et al* point out that there have not been previous theoretical attempts at describing the spin-electric effect in systems such as  $Fe^{3+}$  triangular systems.

In this paper we perform calculations on two energetically competitive spin manifolds of the molecule introduced by Boudalis *et al*. In contrast to other molecular magnets that have exhibited either Type-1 or Type-2 be-

havior but not both, our calculated results suggest that this molecule can exhibit both Type-1 and Type-2 behavior. In addition, the occurrence of two different spin manifolds, composed of high and low half-integer triangular spins, yields two different states that both exhibit spin-electric coupling. This behavior is due to nearly degenerate qualitatively different electronic configurations on the  $Fe^{3+}$  ions. To further quantify this result, we perform calculations to determine the splitting between the two sets of Kramer doublets.

One of the ways that high-spin and low-spin systems differ is that when spin-orbit is turned on, there is indeed a difference between a low-moment  $C_3$  system with one unpaired electron on each site and a high-moment  $C_3$  system with five unpaired electrons on each site. The former problem maps onto a standard three-site one-band Heisenberg Hamiltonian and there is only one electron that can hop from one site to the next. However, for a high-moment system, there are several electrons on each site that can hop to other sites. In both high-moment and low-moment cases, these are high-energy charge transfer excitations. Further, for the high-spin case, it is possible, if not likely, that the energy to flip the spin of a single electron on a high-moment site is the lowest electronic excitation in the problem. This is in contrast to the low-moment system where such a flip simply gives a different degenerate configuration. Alternatively, in the limit of a single exchange-coupling parameter and no spin-orbit interaction it can be shown analytically that the lowest energy structure has a spin of  $\frac{1}{2}$ .

## II. THEORY AND METHODOLOGY

The geometry of  $(Fe^{+3})_3O^{-2}(NC_5H_5)_3(O_2CC_6H_5^{-1})_6$  cationic complex is shown in Fig. 1. The point group symmetry of this molecule has twelve symmetry operations. When oriented so that the  $\langle 111 \rangle$  axis is along the cylindrical axis, the group may be generated from cyclic permutations,  $(x, y, z) \rightarrow (z, x, y)$ , an inverted non-cyclic permutation  $(x, y, z) \rightarrow (-y, -x, -z)$  and the special rotation matrix,  $R_Q$  below:

$$R_Q \equiv \begin{pmatrix} \frac{1}{3} & -\frac{2}{3} & -\frac{2}{3} \\ -\frac{2}{3} & \frac{1}{3} & -\frac{2}{3} \\ -\frac{2}{3} & -\frac{2}{3} & \frac{1}{3} \end{pmatrix}$$

The matrix that we call  $R_Q$  has interesting properties which we want to point out in the event there is deeper relevance. One third of the matrix elements have a magnitude of  $1/3$ . Two thirds of the matrix elements have a

TABLE I: Atomic positions, local charges and local moments for the inequivalent atoms for the low-moment and high-moment configurations of the molecule. The number of decimal places included in the table is technically necessary, with respect to round-off error, if one wishes to use all 12 symmetry operations that this molecule has. The local charges for the first nearest-neighbor oxygens, the nitrogens and the iron atom are very sensitive to the total spin as is the local charge on the Fe iron. The columns presenting the local charges and local moments provide the integrated density ( $\rho$ ) or spin density ( $\rho_{\uparrow} - \rho_{\downarrow}$ ) within a sphere with a physically determined radius around each atom and are provided to qualitatively show differences in the number of unpaired electrons and/or charge on each atomic site. The sphere radii, in Bohr, used for the table are 0.57, 1.46, 1.32 1.24 and 2.19 for H, C, O, N and Fe respectively.

Atom( $M_S = 3/2$ )	X (Bohr)	Y (Bohr)	Z (Bohr)	Charge	Moment ( $\mu_B$ )	Bond $_{Fe-X}$ (Bohr)
Fe <sub>1</sub>	-2.505257638898	0.000000000000	2.505257638898	<b>24.6076</b>	<b>-0.9059</b>	6.14
O <sub>1</sub>	-0.000000000000	-0.000000000000	0.000000000000	5.8622	<b>-0.1589</b>	3.54
O <sub>2</sub>	5.322330564106	-0.260403104702	-0.569772212054	5.9732	<b>-0.0081</b>	3.65
N <sub>1</sub>	-5.469739941306	0.000000000000	5.469739941306	5.1263	<b>0.0089</b>	4.19
H <sub>1</sub>	11.304895903521	-6.589849613853	2.357523144834	0.1674	0.0000	
H <sub>2</sub>	7.864556395661	-3.362449434801	2.251053480429	0.1688	0.0001	
H <sub>3</sub>	10.683035052801	-10.683035052801	0.000000000000	0.1680	0.0000	
H <sub>4</sub>	-6.543623208391	-6.620545602585	3.489866469741	0.1684	-0.0000	
H <sub>5</sub>	-8.368306728391	-10.916470039662	4.136202388450	0.1682	0.0000	
H <sub>6</sub>	14.719044124807	5.924135872740	-2.870772379330	0.1680	-0.0000	
C <sub>1</sub>	9.575468406012	-6.966039283004	1.304714561505	4.5269	0.0004	
C <sub>2</sub>	7.998708653694	3.103090515412	-1.792527622874	4.5186	0.0005	
C <sub>3</sub>	12.837466637187	5.150605294141	-2.536256048906	4.5148	0.0004	
C <sub>4</sub>	5.426718397270	1.954961030125	-1.516796337019	4.5631	0.0040	
C <sub>5</sub>	10.159365328460	1.761777636054	-1.028346613212	4.5154	0.0008	
C <sub>6</sub>	-6.513151601449	-10.695846403617	3.264169130844	4.5196	-0.0003	
C <sub>7</sub>	9.229044950899	-9.229044950899	-0.000000000000	4.5170	0.0007	
C <sub>8</sub>	7.662136522555	-5.149561540879	1.256287490837	4.5224	0.0009	
Atom( $M_S = 15/2$ )	X	Y	Z	Charge	Moment	Bond $_{Fe-X}$
Fe <sub>1</sub>	-2.624000490437	0.000000000000	2.624000490437	<b>24.1523</b>	<b>-4.0536</b>	6.42
O <sub>1</sub>	-0.000000000000	-0.000000000000	-0.000000000000	5.8806	<b>-0.4721</b>	3.71
O <sub>2</sub>	5.546433265240	-0.133871508300	-0.584097636058	5.9742	<b>-0.0924</b>	3.88
N <sub>1</sub>	-5.616413919617	0.000000000000	5.616413919617	5.1416	<b>-0.0480</b>	4.23
H <sub>1</sub>	11.439260476625	-6.717843055563	2.360708710532	0.1672	-0.0001	
H <sub>2</sub>	7.976303528027	-3.475887148864	2.250208189581	0.1684	-0.0004	
H <sub>3</sub>	10.802377433120	-10.802377433120	-0.000000000000	0.1673	-0.0000	
H <sub>4</sub>	-6.628367099071	-6.865310123732	3.552728696144	0.1681	-0.0000	
H <sub>5</sub>	-8.468314677454	-11.157230645789	4.201071032716	0.1682	-0.0000	
H <sub>6</sub>	14.965631738810	6.046722331729	-2.872187075351	0.1682	0.0000	
C <sub>1</sub>	9.705086882387	-7.083371945982	1.310857468206	4.5285	-0.0027	
C <sub>2</sub>	8.260207170085	3.208484962171	-1.843237245734	4.5238	-0.0118	
C <sub>3</sub>	13.086116921516	5.256980392042	-2.572156137428	4.5126	-0.0024	
C <sub>4</sub>	5.689882020246	2.067341855194	-1.555198309861	4.5576	-0.0099	
C <sub>5</sub>	10.415707071475	1.859209556094	-1.086370094156	4.5170	-0.0022	
C <sub>6</sub>	-6.616817839121	-10.946476994912	3.318646821096	4.5202	-0.0003	
C <sub>7</sub>	9.343716620569	-9.343716620569	-0.000000000000	4.5117	-0.0004	
C <sub>8</sub>	7.795420503774	-5.271264738051	1.262077882858	4.5261	-0.0023	

magnitude of  $2/3$ . The sum of each row is  $-1$ . The sum of each column is  $-1$ . The sum of the diagonal elements is  $1$ . The matrix is the transpose of itself and is also its own inverse. The determinant of the matrix is  $-1$  which is of course expected of a matrix-representation of a symmetry operation. The determinant of any  $2 \times 2$  minor matrix is either  $1/3$  or  $-2/3$ . The eigenvalues of this symmetric matrix all have a magnitude of  $1$  with  $1/3$  of the eigenvalues

being negative and  $2/3$  of the eigenvalues being positive.

The resulting group of order  $12$  leads to a total of six representations with degeneracies of  $(1,1,2,2,1,1)$ . None of these representations are either even or odd under inversion. For an isolated  $Fe^{+3}$  atom, the ground state of the system has an outer valence configuration of  $3d^{\uparrow\uparrow\uparrow\uparrow}$  leading to a high net spin of  $S = 5/2$ . However, a higher energy configuration of  $3d^{\uparrow\uparrow}3d^{\downarrow\downarrow}$  with a low net spin

of  $S = 1/2$  is also electronically and magnetically stable but approximately 2-3 eV higher in energy than the high-spin  $Fe^{+3}$  cation. Our results indicate that when ligated according to the figure, the relative stability of the high- and low-spin is changed significantly. In Table I we present the local charges and moments for each of the inequivalent atoms that we have found in calculations for the high- and low- moment manifolds. We also compare the five Fe-O and Fe-N nearest-neighbor distances for the two structures.

The calculations presented here use approximations to density-functional theory (DFT) [28–30], at the generalized-gradient level, to describe the electronic and magnetic structure of the molecular cation. The NRL-MOL computational code employs Gaussian orbitals to represent the Kohn-Sham orbitals. [31–33] The basis sets that are used in NRLMOL are roughly triple to quadruple zeta quality [33]. The PBE-GGA density functional approximation is used for the exchange correlation functional in these self-consistent-field (SCF) calculations. For the iron atom, we have used 20 bare Gaussians with exponents varying from 0.12050 to  $0.38667 \times 10^7$  to construct a contracted basis set composed of 7 s-type, 5 p-type, and 4 d-type contracted orbitals. For simplicity in describing the basis sets on other atoms we refer to this as [Fe(20): 0.12050 –  $0.38667 \times 10^7$ , 7s5p4d]. With this notation the oxygen, nitrogen, carbon, and hydrogen basis sets are designated as: [O(13): 0.10492 –  $0.61210 \times 10^5$ , 5s4p3d], [N(13): 0.09411 –  $0.51751 \times 10^5$ , 5s4p3d], [C(12): 0.07721 –  $0.22213 \times 10^5$ , 5s4p3d] and [H(6): 0.22838 –  $0.77840 \times 10^2$ , 4s3p1d] respectively. The Limited-Memory Broyden-Fletcher-Goldfarb-Shanno (LBFGS) scheme programmed by Liu and Nocedal [34] has been used for the optimization of structure with energy and force convergence criteria of  $0.10000 \times 10^{-5}$  Hartree and .003 Hartree/Bohr for consistency.

Spin polarized calculations have been performed with the inclusion of spin-orbit coupling for the evaluation of magnetic properties [11].

### III. RESULTS AND ANALYSIS

Generally speaking, to determine the relevant parameters for the spin Hamiltonians for a triangular lattice of identical spins ( $S_{loc}=1/2$  or  $5/2$  here), one calculates the energy of the ferromagnetically ordered state  $E^{FM}$  and the anti-ferromagnetically ordered state  $E^{AF}$ . Then based on the assumption of a Heisenberg Hamiltonian of the form  $H = E_o + J[\mathbf{S}_1 \cdot \mathbf{S}_2 + \mathbf{S}_2 \cdot \mathbf{S}_3 + \mathbf{S}_3 \cdot \mathbf{S}_1]$ , one can determine that  $E_o = (E^{FM} + 3E^{AF})/4$  and  $J = (E^{FM} - E^{AF})/(4S_{loc}^2)$ . For our calculations, we find energies of  $E^{FM}(S_{loc} = 1/2) = -7129.712342$  and  $E^{FM}(S_{loc} = 5/2) = -7129.697517$  Hartree. For each of these cases we then calculate the antiferromagnetically ordered structures finding energies of  $E^{AF}(S_{loc} = 1/2) = -7129.714280$  and  $E^{AF}(S_{loc} = 5/2) = -7129.714586$

Hartree. After extracting  $E_o$  and  $J$  for both the high-spin and low-spin configurations we can arbitrarily shift both spin Hamiltonians by a constant so that  $E_o(S_{loc} = 1/2) \equiv 0$ . The resulting values of  $J$  and  $E_o$  are given in Table II. This Heisenberg Hamiltonian may be more simply represented according to:

$$H = E_o(S_{loc}) + \frac{J}{2}\{\sum_i \mathbf{S}_i^2 - \sum_i S_i^z\}. \quad (1)$$

The resulting eigenstates of the above Hamiltonian, arising from a specific  $S_{loc}$ , are also eigenstates of  $S_{tot}^2, S_{tot}^z$ . In the absence of anisotropy, the energies are given by

$$E = E_o(S_{loc}) + \frac{J}{2}[S_{tot}(S_{tot} + 1) - 3S_{loc}(S_{loc} + 1)] \quad (2)$$

This affirms that regardless of  $S_{loc}$  the ground-state energy corresponds to  $S_{tot} = 1/2$ . This equation allows us to determine the relative energies of the two sets of Kramer doublets that are associated with the two different spin manifolds. These are presented in the last column of Table II. In Table II we present results for the energies of the high-spin and low-spin manifolds as a function of spin orderings. Also presented in Table II are the magnetic anisotropy energy (MAE) for each spin manifold and the energy gap ( $\Delta^{AF/FM}$ ) between ferromagnetic and antiferromagnetic structures. To definitively affirm our local-spin assignments of  $S=1/2$  and  $S=5/2$  metal-centers and the spin orderings for various calculations, we also present the local moments, labeled  $\mu_i^{AF}$  or  $\mu_i^{FM}$ , in Table II. Confirmation of these assignments are necessary to justify the form of the Heisenberg Hamiltonian we have utilized in this analysis. While the total number (spin moment) of unpaired electrons (3 for the low-spin manifold and 15 for the high-spin manifold) are well defined quantities and indicative of spin  $1/2$  and  $5/2$  metal centers, this additional information is required to unambiguously demonstrate, computationally, that the electrons participating in spin polarization are indeed primarily associated with the metal ions. Our integrated net spins in non-space filling spheres ( $R=2.19$  au) are in the range of  $\mu = 3.84 - 4.04$  and  $\mu = 0.91 - 0.97$  for the high-spin and low-spin systems. The lack of local moments on other sites (See Table I) confirms that the Heisenberg-model employed here is sufficient for the analysis.

As shown in Table II, the dipole moment for the antiferromagnetic high-spin ( $5/2$ ) manifold is larger by a factor of 1.5. In previous papers [20–22] it has been noted that the dipole moment of the generally non-stationary antiferromagnetic state is the key indicator of a good spin-electric system composed of low-spin metal centers. We emphasize that these antiferromagnetic states are only eigenstates of the system in the high-field limit. In addition to differing spin-electric coupling strengths in the low-field limit, this result suggests that the system could be driven from the low-spin to high-spin manifold by application of an electric field. As such this system also presents the possibility for a uni-directional electros-

TABLE II: Magnetic and spin-electric properties for two nearly degenerate spin manifolds of the cation. The first manifold has a local spin and valence of  $1/2 3d^{\uparrow\uparrow\uparrow\downarrow}$  on each Fe ion. The second manifold has a local valence of  $5/2 3d^{\uparrow\uparrow\uparrow\uparrow}$  on each Fe ion. For both cases the energy splitting between the antiferromagnetic and ferromagnetic structure ( $\Delta^{AF/FM}$ ) and the magnetic anisotropy energy (MAE) is given. The spontaneous dipole moments acquired by the antiferromagnetically ordered structures are qualitatively different in magnitude. The calculated local moments (within a sphere of radius 2.19 Bohr) are consistent with the local valences. In both cases, the dipole moments result from movement of electrons from the two ions with paired spins to the ion with an unpaired spin as in the case of Ref. [21]. For calculations of J, we use the convention that the Heisenberg Hamiltonian is given by  $H = E_o + J(\mathbf{S}_1 \cdot \mathbf{S}_2 + \mathbf{S}_2 \cdot \mathbf{S}_3 + \mathbf{S}_3 \cdot \mathbf{S}_1)$ . In other words both manifolds prefer antiferromagnetic ordering.

$S_{loc}$	$E_o$ (eV)	J(eV)	MAE (K)	$\Delta^{AF/FM}$	AF Dipole (au)	$\mu^{FM}$	$\mu_1^{AF}$	$\mu_2^{AF}$	$\mu_3^{AF}$	$E_o + J[\frac{3}{4} - 3S_{loc}(S_{loc} + 1)]$
1/2	0.000	0.053	3.8 (EA)	-0.053	0.091	0.91	0.97	-0.93	-0.93	-0.08 (eV)
5/2	0.095	0.019	-8.5 (EP)	-0.424	0.139	4.05	3.94	-3.84	-3.84	-0.39 (eV)

TABLE III: Energy (eV) of ferromagnetically ordered molecule as a function of  $M_S$  and the geometry. This molecule shows spin crossover behavior as a function of the geometry which suggests that the ground magnetic state will change when pressure is applied and that it could be sensitive to size of the charge-compensating counter anion in the unit cell.

$M_S$	$\Delta E^{3/2}$	$\mu^{3/2}$	$\Delta E^{15/2}$	$\mu^{15/2}$
3/2	0.000	0.91	1.602	0.93
6/2	0.891	1.88	1.792	1.95
9/2	1.277	2.73	1.226	2.82
12/2	1.865	3.45	0.924	3.51
15/2	1.930	4.05	0.404	4.05

tic spin crossover effect that has been discussed earlier in applications to explicitly polar magnetic molecules [35].

There are in fact other spin-ordered solutions, with qualitatively different moments, than discussed in detail here, that we have found during the course of these calculations. Because of this we have performed fixed moment ferromagnetic single-point calculations, as a function of total moment, at the low-spin and high-spin equilibrium geometries. In Table III we present the energies as a function of total moment. The results show that it is indeed only the lowest-spin and highest-spin configurations that are expected to be energetically competitive ground states.

From Table I we observe that a spin moment appears on the central atoms for the high-spin case but not for the low-spin case. This moment has the same sign as the moment on the Fe ions which could simply mean that some of the valence charge on the Fe ions is leaking onto the central oxygen. If this is the case, it could mean that there is a greater degree of Fe  $4s$ - $3d$  hybridization for the case of the high-spin manifold. To make links with future experiments, we provide predictions of the relative energies of the Fe  $1s$  and  $2s$  states and the O  $1s$  states as a function of spin manifold. We find that the Fe  $1s$ -core levels for the high spin manifolds shift downward by 1.4 eV. Similarly the Fe  $2s$  core levels move downward

by approximately 1.4 eV. However, in contrast to the Fe  $1s$ -core levels, the  $2s$ -core levels exhibit a qualitatively different broadening for the two spin manifolds. For the low-spin manifold the width of the Fe  $2s$  core energies is approximately 0.5 eV. But for the high-spin manifold, the broadening increased to 2.2 eV. The broadening is consistent with spin polarization rather than chemical bonding. The oxygen  $1s$  states also show a larger broadening (0.82 vs 0.16 eV) for the case of the high-spin manifold and are shifted upward, rather than downward, by about 0.47 eV relative to the low-spin manifold. A perfect ionic model would predict that the  $1s$  oxygen levels would shift by 1.1 eV if we only consider the change in Coulomb potential due to a +3 Fe cation at the origin. By broadening, we are referring to changes in energies of various core states due to a combination of exchange coupling and geometrical changes in the molecules.

#### IV. SUMMARY

To summarize, the  $\text{Fe}^{III}$  ions, arranged at the vertices of an equilateral triangle, in the cationic molecule studied here can exist with valences of  $3d^{\uparrow\uparrow\uparrow\uparrow}$  or  $3d^{\uparrow\uparrow\uparrow\downarrow}$ . Our geometries, optimized for each spin configuration, find that the lowest energy Kramer doublet states for each system are close in energy but with the high-moment case slightly lower in energy (0.3 eV). Both of these degenerate Kramer doublet states can be manipulated with an electric field. As discussed in Refs. [19, 21, 22, 36, 37], it is generally expected that density-functional methods, without corrections for the onsite Coulomb repulsion, will overestimate exchange-coupling parameters by a factor of 2-3 which would then adjust the energy splitting to a number that is close to room temperature. There are other factors that usually do not enter in to determining the optimal ground-state reference energy that could then play a role in fully determining the splitting between the two sets of Kramer doublets that arise from the two different reference states. Other factors that should be considered include zero-point vibrational energies and average spin-orbit energies. The expectation

is that vibrational effects would slightly stabilize the low-spin manifold and that inclusion of the total spin-orbit energy would slightly favor the high-spin manifold. Work on quantifying this result is in progress.

Regardless of which reference state is lower in energy, the presence of nearly degenerate reference states, composed of high-spin and low-spin centers, is of potential interest for quantum sensing applications. The low-spin case offers the possibility of a molecular magnet that has weak easy-axis anisotropy and that would therefore be switchable through the applications of magnetic fields as well as electric fields. The low-spin and high-spin case offers the possibility of two different spin-electric signatures. Prospects for practically switching between these two states appear to be good. The overall size of the molecular cation depends on the moments which means that the Madelung stabilization of the low-spin molecule, in a crystal, could be greater if counter anions of differing size can be used. In addition to more experiments on this interesting molecular magnetic qubit, it will be important to consider the use of higher-level quantum chemistry methods, and improved density-functional based methods, such as those obtained from the Fermi-Löwdin-Orbital-Self-Interaction-Corrected (FLOSIC) [38–45]. Finally the inclusion of non-collinear mean-field methods, with comparison to

multiconfigurational methods, will help to realize quantitative computational understanding of this qubit. Due to the importance of rigorously understanding decohering mechanisms in these systems, inclusion of group-theoretical symmetrization methods have been used here. Fully incorporating such techniques into non-collinear and multi-configurational approaches should enhance the effectiveness for applications to quantum sensors and qubits.

## V. ACKNOWLEDGEMENTS

A.I. Johnson thanks the Michigan-State Computer Center for computer time used on this project. M.R.P. was supported from startup funds provided by the University of Texas-El Paso and the Texas Science and Technology Acquisition and Retention (STARS) Program. CMC and FI are supported by the Faculty of Technology at Linnaeus University, the Swedish Research Council (VR) through Grant No. 621-2014-4785, and by the Carl Tryggers Stiftelse through Grant No. CTS 14:178. Computational resources for preliminary calculations have been provided by the Lunarc Center for Scientific and Technical Computing at Lund University.

- 
- [1] Najafpour, M. M., Renger, G., Hoiyniska, M., Moghadam, A. N., Aro, E-M., Carpentier, R., Nishihara, H., E-Rye, J. J., Shen, J.R. and Allakhverdiev, S. I. **Manganese Compounds as Water-Oxidizing Catalysts: From the Natural Water-Oxidizing Complex to Nanosized Manganese Oxide Structures**, Chem. Rev. **116**, 2886-2936 (2016).
- [2] Glueckner, C., Kern, J., Brose, M., Zouni, A., Yachandra, V. and J. Yano. **Structural Changes of the Oxygen-evolving Complex in Photosystem II during the Catalytic Cycle**. J. Biol. Chem. **288**, 22607-22620 (2013).
- [3] H. Dau, and M. Haumann, **The manganese complex of photosystem II in its reaction cycle Basic framework and possible realization at the atomic level**, Coord. Chem. Rev. **252**, 273-295 (2008).
- [4] G. Christou, J. B. Vincent, J.S. Bashkin, C. Christmas, and J.C. Huffman, **Synthesis of Tetranuclear Manganese Complexes as Models of the Photosynthetic Water Oxidation Site**, Rec. Trav. Chim. Pays. Bas. **106**, 217 (1987).
- [5] J. Batool, T. Hahn, and M.R. Pederson, **Magnetic Signatures of Hydroxyl- and Water-Terminated Neutral and Anionic Mn<sub>12</sub>-Acetate**, J. Comput. Chem. **26** 2301-2308 (2019).
- [6] D.I. Khomskii, **Electric dipoles on magnetic monopole in spin ice** Nature Comm. **3** 904 (2012).
- [7] M.N. Leuenberger and D. Loss, **Quantum computing in molecular magnets**, Nature **410**, 789-793 (2001).
- [8] B. Georgeot and F. Mila, **Chirality of Triangular Antiferromagnetic Clusters as a Qubit**, Phys. Rev. Lett. **104**, 200502 (2010).
- [9] **Molecular electronic spin qubits from a spin-frustrated trinuclear copper complex** B. Kintzel, M. Bohme, J.J. Liu, A. Burkhardt, J. Mrozek, A. Buchholz, A. Ardavan, W. Plass, CHEMICAL COMMUNICATIONS, **54**, 12934 (2018). DOI: 10.1039/c8cc06741d (2018).
- [10] M.R. Pederson, and S.N. Khanna, **Magnetic Anisotropy Barrier For Spin Tunneling in Mn<sub>12</sub>O<sub>12</sub> Molecules**, Phys. Rev. B. **60**, 9566-9572 (1999).
- [11] M.R. Pederson, and S.N. Khanna, **Electronic Structure and Magnetism of Passivated MnO Nanomagnets** Chem. Phys. Lett. **307**, 253-258 (1999).
- [12] L. Thomas, F. Lioni, R. Barrou, D. Gatteschi, R. Sessoli, and B. Barbara, **Macroscopic quantum tunnelling of magnetization in a single crystal of nanomagnets**, Nature **383**, 145 (1996).
- [13] J.R. Friedman, M.P. Sarachik, J. Tejada, and R. Ziolo, **Macroscopic measurement of resonant magnetization tunneling in high-spin molecules** Phys. Rev. Lett. **76**, 3830 (1996).
- [14] C.V. Wullen, **Magnetic Anisotropy From Density Functional Calculations. Comparison of Different Approaches: Mn<sub>12</sub>O<sub>12</sub>-Acetate as a Test Case** J.Chem. Phys. **130**, 194109 (2009).
- [15] S. Schmitt, P. Jost, and C.V. Wullen, **Zero-field splittings from density functional calculations: Analysis and improvement of known methods** J. Chem. Phys. **134**, 194113 (2011).
- [16] L. Michalak, C.M. Canali, M.R. Pederson, M. Paulsson,

- and V.G. Benza, **Theory of Tunneling Spectroscopy in a Mn<sub>12</sub> Single-Electron Transistor by Density-Functional Theory Methods**, Phys. Rev. Lett. **104**, 017202,1-4 (2010).
- [17] J.F. Nossa, M.F. Islam, C.M.Canali, and M.R. Pederson, **Electric control of the Fe<sub>4</sub> single-molecule magnet in a single electron transistor**, Phys. Rev. B **88**, 224423 (2013).
- [18] K.-Y. Choi, H. M. Yasuhiro, N. Hiroyuki, U. Kortz, F. Hussain, A.C. Stowe, C. Ramsey and N.S. Dalal, **Observation of Half Step Magnetization in the Cu<sub>3</sub>-Type Triangular Spin Ring**, Phys. Rev. Lett. **96**, 207202 (2006).
- [19] J. Kortus, C.S. Hellberg and M.R. Pederson, **Hamiltonian of the V<sub>15</sub> spin system from first principles**, Phys. Rev. Lett. **86**, 3400-3403 (2001).
- [20] M. Triff, F. Troiani, D. Stepanenko, and D. Loss, **Spin Electric Coupling in Molecular Magnets**, Phys. Rev. Lett. **101**, 2)17201 (2008).
- [21] M.F. Islam, Javier F. Nossa, Carlo M. Canali, and Mark Pederson. **First-principles study of spin-electric coupling in a Cu<sub>3</sub> single molecular magnet**, Phys. Rev. B **82**, 155446,1-9 (2010).
- [22] J.F. Nossa, M.F. Islam, C.M. Canali, and M.R. Pederson, **First-principles studies of spin-orbit and Dzyaloshinskii-Moriya interactions in the Cu<sub>3</sub> single-molecule magnet**, Phys. Rev. B **85**, 085427,1-9 (2012).
- [23] A.K. Boudalis, J. Robert and P. Turek, **First Demonstration of Magnetoelectric Coupling in a Polynuclear Molecular Nanomagnet: Single-Crystal EPR Studies of [Fe<sub>3</sub>O(O<sub>2</sub>CPh)<sub>6</sub>(Py)<sub>3</sub>](ClO<sub>4</sub>)<sub>3</sub>·Py under Static Electric Fields**, Chem. Eur. J. **24**, 14896-14900 (2018).
- [24] **Electric Field Control of Spins in Molecular Magnets** JJ Liu, J. Mrozek, W.K. Myers, G.A. Timco, R.E.P. Winpenny, B. Kintzel, W. Plass, A. Ardavan, Phys. Rev. Lett., **122**, 027202, DOI: 10.1103/PhysRevLett.122.037202 (2019).
- [25] **Determination of the Distributions of the Spin-Hamiltonian Parameters in Spin Triangles: A Combined Magnetic Susceptometry and Electron Paramagnetic Resonance Spectroscopic Study of the Highly Symmetric [Cr<sub>3</sub>O(PhCOO)<sub>6</sub>(py)<sub>3</sub>](ClO<sub>4</sub>)<sub>3</sub> center dot 0.5py** A.K. Boudalis, G Rogez, P Turek, INORGANIC CHEMISTRY, **57**, 13249-13269 (2018). DOI: 10.1021/acs.inorgchem.8b01764
- [26] I. Dzyaloshinsky, **A thermodynamic theory of "weak" ferromagnetism of antiferromagnetics**, J. Phys. and Chem. of Sol. **4** 241-255 (1958).
- [27] T. Moriya, **New mechanism for anisotropic superexchange interaction**, Phys. Rev. Lett. **4**, 228 (1960).
- [28] Y. Wang and J.P. Perdew, **Spin scaling of the electron-gas correlation energy in the high-density limit** Phys. Rev. B **43**, 8911 (1991).
- [29] J.P. Perdew, J.A. Chevary, S.H. Vosko, K.A. Jackson, M.R. Pederson, D.J. Singh, and C. Fiolhais, **Atoms, Molecules Solids and Surfaces: Applications of the Generalized Gradient Approximation for Exchange and Correlation**, Phys. Rev. B **46**, 6671-6687 (1992).
- [30] J.P. Perdew, K. Burke, and M. Ernzerhof, **Generalized Gradient Approximation made Simple** Phys. Rev. Lett. **77**, 3865-3868 (1996).
- [31] M.R. Pederson, and K.A. Jackson, **Variational Mesh for Quantum-Mechanical Simulations**, Phys. Rev. B. **41**, 7453-7461 (1990).
- [32] K.A. Jackson, and M.R. Pederson, **Accurate Forces in a Local-Orbital Approach to the Local Density Approximation**, Phys. Rev. B. **42**, 3276 (1990).
- [33] D.V. Porezag and M.R. Pederson, **Optimization of Gaussian-Basis Sets for Density Functional Calculations**, Phys. Rev. A. **60**, 2840-2847 (1999).
- [34] D. Liu, and J. Nocedal, **On the limited memory BFGS method for large-scale optimization**, Math. Prog. B. **45**, 503-528 (1989).
- [35] N. Baadji, M. Piancenza, T. Tugsuz, F. D. Sala, G. Maruccio and S. Sanvito, **Electrostatic spin crossover effect in polar magnetic molecules**, Nature Materials **8**, 813-817 (2009).
- [36] E. Ruiz, A. Rodriguez-Forteza, J. Cano, S. Alvarez and P. Alemany, **About the calculation of exchange coupling constants in polynuclear transition metal complexes**, J. Comp. Chem. **24**, 982-989 (2003).
- [37] K. Park, M.R. Pederson and C.S. Hellberg, **Properties of low-lying excited manifolds in Mn<sub>12</sub> acetate**, Phys Rev. B **69**, 014416 (2004).
- [38] M.R. Pederson, A. Ruzsinszky, and J.P. Perdew, **Communication: Self-interaction correction with unitary invariance in density functional theory**, J. Chem. Phys. **140**, 121103,1-4 (2014).
- [39] M.R. Pederson, **Fermi orbital derivatives in self-interaction corrected density functional theory: Applications to closed shell atoms**, J. Chem. Phys. **142**, 064112,1-7 (2015).
- [40] Z.H. Yang, M.R. Pederson, and J. P. Perdew, **Full self-consistency in Fermi-orbital self-interaction correction** Phys. Rev. A. **95**, 052505 (2017).
- [41] D.-Y. Kao, K. Withanage, T. Hahn, J. Batool, J. Kortus, and K.A. Jackson, **Self-consistent self-interaction corrected density-functional theory calculations atoms using Fermi-Löwdin orbitals: Optimized Fermi-orbital descriptors for Li-Kr**, J. Chem. Phys. **147** 164107 (2017).
- [42] D.-Y. Kao, and M.R. Pederson, **Use of Löwdin orthogonalised Fermi orbitals for self-interaction corrections in an iron porphyrin**, Mol. Phys. **115**, 552 (2017).
- [43] T. Hahn, S. Liebing, J. Kortus, and M.R. Pederson, **Fermi orbital self-interaction corrected electronic structure of molecules beyond local density approximation**, J. Chem. Phys. **143**, 224104,1-7 (2015).
- [44] M.R. Pederson, T. Baruah, D.-Y. Kao, and L. Basurto, **Self-interaction corrections applied to Mg-porphyrin, C<sub>60</sub>, and pentacene molecules**, J. Chem. Phys. **144**, 164117,1-8 (2016).
- [45] R. P. Joshi, K. Trepte, K.P.K. Withanage, K. Sharkas, Y. Yamamoto, L. Basurto, R.R. Zope, T. Baruah, K.A. Jackson and J.E. Peralta, **Fermi-Löwdin orbital self-interaction correction to magnetic exchange couplings** J. Chem. Phys. **149**, 164101 (2018).